Research Square

Preprints are preliminary reports that have not undergone peer review.
They should not be considered conclusive, used to inform clinical practice,
or referenced by the media as validated information.

Lignin–alginate biohydrogels for controlled release of triple superphosphate in circular agroecosystems

Tarun Kumar Gayen
Delhi Technological University, India
Mohammad Amdad Ali
Illinois Materials Research Laboratory, University of Illinois at Urbana-Champaign, Urbana, Illinois 61801, USA
Sudhir G Warkar
sgwarkar@dtu.ac.in

Delhi Technological University, India

Research Article

Keywords: Agricultural waste, Circular economy, Lignin, Sodium alginate, Hydrogel, TSP, Nutrient release

Posted Date: August 5th, 2026

DOI: https://doi.org/10.21203/rs.3.rs-9807570/v1

License: This work is licensed under a Creative Commons Attribution 4.0 International License.
Read Full License

Additional Declarations: No competing interests reported.

Abstract

Conventional fertilization practices in agriculture are being replaced by more convenient and sustainable technologies, driven by the discovery of controlled- and slow-release fertilizers, to reduce pollution by upcycling agricultural waste and to ensure food security for the global population through effective waste management. The use of biopolymers in developing fertilization technology has evolved to address challenges in farming practices. In this study, lignin, a bio-polymer isolated from agricultural waste, mustard straw, was combined with another biopolymer, sodium alginate (SA), to prepare a bio-hydrogel. The SA-lignin (1:1) hydrogel was used to control the release of fertilizer, specifically triple superphosphate (TSP). The TSP release in water and soil using the SA-lignin hydrogel as a fertilizer carrier was monitored in two different ways. Firstly, TSP was loaded into the SA-lignin hydrogel using the in-situ method, and its release was evaluated using empirical kinetic models. Secondly, TSP fertilizer was coated/encapsulated in SA-lignin hydrogel, and its release was studied using empirical kinetic models. However, TSP-loaded SA-lignin hydrogel samples showed cumulative phosphorus release of ~ 92% after 20 days in DI water and ~ 77% after 40 days in soil. TSP-coated fertilizer showed cumulative phosphorus release of ~ 95% after 10 days in water and ~ 88% after 22 days in soil. The SA-lignin hydrogel is convenient for loading and coating with TSP, resulting in slower phosphorus release than pure TSP, which releases 100% of its phosphorus within 24 h. This highlights the potential of SA-lignin hydrogel for controlled nutrient release in sustainable agricultural practices, thereby minimizing environmental pollution.

1. Introduction

Rapid population growth and economic expansion have intensified energy demand, resource depletion, and environmental pollution. Transitioning toward a circular economy requires the upcycling of agricultural residues into value-added products [1]. Such residues are rich in renewable biomass components, including cellulose, hemicellulose, lignin, and pectin [2]. Among these, mustard straw is a major yet underutilized by-product, with India generating approximately 23.4 million tons annually, nearly 75% of which remains unused [3]. As lignocellulosic biomass, mustard straw represents a valuable source of lignin—the second most abundant biopolymer after cellulose [4]. Industrial lignin is also generated in large quantities, but only a small fraction is valorized into products such as phenolic resins, adhesives, carbon fibers, activated carbon, dispersants, and antioxidants [4].

While cellulose-based hydrogels are widely used for controlled fertilizer release and soil water retention, direct application of lignin in hydrogels is limited due to its predominantly hydrophobic and rigid aromatic structure [5]. Its backbone, composed of non-polar phenylpropane units, restricts water interaction despite the presence of hydroxyl groups [4]. The highly crosslinked three-dimensional network, stabilized by strong carbon–carbon and ether linkages, hydrogen bonding, and π–π interactions, imparts mechanical strength but limits flexibility and water uptake [4]. To enhance its agricultural applicability, lignin is commonly blended with hydrophilic polymers. Lignin-based hydrogels with hydrophilic polymers exhibit high water uptake and tuneable swelling, suitable for controlled-release

applications [6]. For example, sodium alginate–lignin coated fertilizers crosslinked with epichlorohydrin achieved sustained urea and phosphorus release (83.57% after 38 days and 82.07% after 40 days, respectively in water) due to dense covalent crosslinking [7]. Similarly, epichlorohydrin-crosslinked alginate/lignin hydrogels showed ~ 50% enhanced structural stability under physiological conditions [8]. However, the toxicity of epichlorohydrin and potential residual presence limit its agricultural use. Bio-based ionic crosslinking strategies, such as incorporating Ca^{2+}-modified montmorillonite, allow "egg-box" junctions with alginate chains, producing hydrogels with reversible ionic crosslinks and ~ 24% phosphorus release after 3 days [9].

Building on this background, we developed a fully biopolymer hydrogel derived from mustard straw lignin and sodium alginate (SA), without external crosslinkers. Lignin is dissolved in NaOH, where phenolic hydroxyl groups deprotonate to form resonance-stabilized phenoxide ions, enhancing solubility and dispersibility. Sodium alginate, an anionic polysaccharide composed of β-D-mannuronic (M) and α-L-guluronic (G) acid residues, is fully deprotonated in basic media, yielding carboxylate ions ($–COO^–$) along the polymer backbone [10]. The resulting electrostatic repulsion prevents network formation, producing a viscous polyelectrolyte solution. Hydrogel formation is triggered by adjusting the pH toward neutral, which reduces repulsion and allows hydrogen bonding, hydrophobic interactions between lignin aromatic domains, and polymer chain entanglement, resulting in a physically crosslinked, environmentally compatible network with good flexibility and water retention. Furthermore, to demonstrate slow release of nutrient, triple superphosphate (TSP, $Ca(H_2PO_4)_2{\cdot}H_2O$) was used for both in situ loading and surface coating. In aqueous conditions, it is expected that Ca^{2+} ions act as ionic crosslinkers between negatively charged polymer sites and phosphate ions (predominantly $H_2PO_4^-$ at neutral pH), stabilizing the hydrogel and modulating phosphorus release. During coating, similar Ca^{2+}–polymer interactions form a stable hydrogel layer around TSP granules, enabling controlled nutrient diffusion.

This study demonstrates a fully biopolymer approach to producing SA–lignin hydrogels for soil hydration and sustained nutrient release, targeting arid and semi-arid regions. Lignin was extracted via alkaline treatment and characterized using FTIR, SEM, DSC, and TGA. The SA–lignin hydrogel was evaluated for structural, thermal, swelling, and water-retention properties. Phosphorus release from TSP-loaded and TSP-coated hydrogels was systematically studied and modelled using empirical kinetic equations, confirming the system's potential as a sustainable, environmentally friendly controlled-release fertilizer platform aligned with circular bioeconomy principles and the United Nations Sustainable Development Goals (SDG 7, 12, and 13) [11, 12].

2. Experimental section

2.1. Materials and chemicals

Mustard straw was collected from the Department of Horticulture, Delhi Technological University, Delhi. Sodium alginate (sodium polymannuronate) (91%), low viscosity (4–12 mPa.s, 1% in H_2O (25 ^oC) with the weight average molecular weight of 233000 $g{\cdot}mol^{-1}$ was purchased from Thermo Fisher Scientific,

Delhi, India. Sodium hydroxide (98%), hydrochloric acid (37%), epichlorohydrin (ECH) (98%), and hexane were purchased from Thermo Fisher Scientific, Delhi, India. Triple superphosphate (TSP), a granular phosphate fertilizer (46% P_2O_5), was purchased from the local market, Rohini, Delhi. All reagents used in this study were of an analytical grade and used without purification. Deionized (DI) water was utilized in all the experiments. The viscosity-average molecular weight (M_η) of mustard straw derived-lignin was determined using an Ostwald viscometer at 25 ^oC to be 27,725 g·mol^{-1} according to Mark–Houwink–Sakurada equation [13].

2.2. Extraction and isolation of lignin

The lignin was extracted from mustard straw by the alkaline method with slight modifications [4]. The mustard straw was cleaned with DI water and dried in air for 72 h. The dry mustard straw was mangled. The crushed mustard straw was sieved through mesh net of 300 µm resulting particle size ~ 300 µm. Then the mustard straw was treated with 0.1 M NaOH at 50 ^oC for 72 h with stirring of ~ 1800 rmp. The solid-liquid ratio was 1:20. It was filtered, and the filtrate was collected for lignin extraction. The filtrate (liquor) was adjusted to a pH of 5.5 using hydrochloric acid (HCl). Precipitation was formed, containing hemicellulose. It was filtered, and the filtrate was collected. The solid residues contain cellulose and hemicellulose. The filtrate was heated at 50 ^oC for 12 h and adjusted to pH 2 using HCl. Solid yellowish-brown lignin was formed and washed with DI water and hexane to remove organic impurities. The lignin was dried in a hot air oven at 40 ^oC for 24 h and stored for further study.

2.3. Purification of lignin

A certain amount of extracted lignin was dissolved in aqueous NaOH solution. After dissolution, HCl was added slowly while adjusting the pH to 2. It was incubated for 24 h for precipitation formation. Precipitation was centrifuged and washed properly with DI water. Then it was washed with hexane to remove fat-containing materials. The solid brown precipitation was dried in a hot air oven at 40 ^oC for 24 h.

2.4. *Calculation of lignin yields*

The lignin yield was calculated by the following equation.

$$Lignin\ yield\ (\%) = \frac{L_1}{L_2} \times 100$$

1

……..

Where L_1 is the weight of the recovered lignin, and L_2 is the weight of the mustard straw used for the extraction.

2.5. Preparation of lignin hydrogel

Lignin hydrogel was prepared by following the chemical crosslinking method with slight modifications [4]. A certain amount of pulverized lignin (1.0 g) with NaOH (0.6 g) was dissolved in DI water (10 mL) by stirring for 48 h at room temperature (25 ^{O}C). The crosslinker epichlorohydrin (2 mL) was added dropwise to the lignin solution and stirred for 24 h at 40 ^{O}C. The lignin is crosslinked with epichlorohydrin, and subsequently, a lignin hydrogel was formed. The lignin hydrogel was incubated for 48 h at room temperature (25 ^{O}C) and washed with DI water to remove unreacted chemicals. Then the lignin hydrogel was dried in a hot air oven at 50 ^{O}C to prepare the dry hydrogel.

2.6. Preparation of SA-lignin hydrogel

Dry lignin of 0.6 g was dissolved in 10 mL 1 M NaOH solution by stirring for 12 h at room temperature (25 ^{O}C). A 0.6 g of SA was dissolved in 10 mL DI water and stirred continuously for 6 h at room temperature (25 ^{O}C). Then 2 mL of lignin solution added dropwise to the SA solution with stirring continuously for 1 h at room temperature (25 ^{O}C). The SA-lignin mixture was poured into a petri dish and incubated for 48 h to form a hydrogel at room temperature (25 ^{O}C). Finally, the SA-lignin hydrogel was dried in a hot air oven at 40 ^{O}C. The SA is physically crosslinked with lignin through interactions between polymers, and hydrogen bonds form between the lignin polymer and the SA polymer. Thus, a three-dimensional complex SA-lignin hydrogel was formed (Fig. 1a-d).

It is worth noting that the mass ratios of lignin to sodium alginate (Table 1) are comprehensively optimized to obtain the optimal preparation conditions of lignin-sodium alginate bio-composite hydrogel. Based on swelling and structural integrity, lignin (0.6 g) and sodium alginate (0.6 g) was chosen for coating/in-situ loading of TSP.

Table 1
Optimization of lignin and SA for the formation of SA-lignin hydrogel. 1 M NaOH solution was used for the SA-lignin hydrogel.

Lignin (g)	SA (g)	Swelling capacity (%)
0.6	0.7	3593
0.6	0.6	3702
0.6	0.5	3612
0.6	0.4	3154
0.6	0.3	2528

2.7. Preparation of TSP fertilizers loaded with SA-lignin hydrogel

TSP was loaded into the SA-lignin hydrogel by the in-situ technique [14]. Lignin (0.6 g), SA (0.6 g), and NaOH (0.4 g) were dissolved in 10 mL of DI water. Then 2.52 g TSP (powder) was added into the SA-

lignin solution, and stirred constantly for 12 h at room temperature (25 ^{o}C). The TSP-SA-lignin was poured into a petri dish and incubated for 72 h for hydrogel formation. The TSP-loaded SA-lignin was dried in a hot air oven at 40 ^{o}C for 48 h.

2.8. Preparation of TSP-coated fertilizers

The TSP fertilizer granules, with a diameter of ~ 2 mm, were selected for coating. The homogeneous TSP granules, weighing 50 g, were placed in a beaker, and the beaker was then positioned on a magnetic stirrer. Then the SA-lignin (1:1) jelly solution was added dropwise by using a dropper. The TSP granules were stirring very slowly, and the SA-lignin solution was added to the beaker slowly. The granules were dried at 40 ^{o}C, and again, SA-lignin jelly solution was added dropwise and dried. The process was repeated three times. The drying time of each coating was 20 min. The coating efficiency was 67% (weight of coating material/weight of fertilizer). Finally, the granules of TSP fertilizers were dried in a hot air oven at 40 ^{o}C.

2.9. Phenolic hydroxyl group content in lignin and hydrogel sample

A 10 mg lignin sample was dissolved in 5 mL of dioxane and 5 mL of 0.2 M NaOH solution separately. Then, 2 mL was taken from each solution and diluted to 25 mL using pH 6 buffer solution and pH 12 buffer solution. The final concentration of each solution was measured to be ~ 0.08 g/L. UV spectra were recorded at 300 and 350 nm using a UV spectrometer (SHIMADZU UV-1900i) with a pH 6 lignin solution as a reference, and the two alkaline solutions were measured against it. These absorbance values were used to determine the amount of phenolic hydroxyl groups in lignin [15].

The amounts of phenolic hydroxyl groups in lignin hydrogel, SA-lignin hydrogel, and TSP-SA-lignin hydrogel were measured by the following procedure. The dry powdered hydrogel samples (10 mg) were separately submerged in dioxane and a 0.2 M NaOH solution. The mixtures were stirred for 24 h at room temperature (25 ^{o}C) and filtered. Then, the content of phenolic hydroxyl groups was measured following the same procedure as described above.

2.10. Fourier Transform Infrared Spectroscopy (FTIR)

The FTIR spectra of the samples were recorded using an FTIR spectrometer (PerkinElmer version 10.5.3) equipped with an attenuated total reflectance (ATR) unit (Pro One sensor). The background spectrum was run initially to subtract it from the resulting spectrum. The spectra were obtained with a resolution of 4 cm^{-1} in transmittance mode, spanning the range of 500 to 4000 cm^{-1}.

2.11. Thermogravimetric analysis (TGA)

TGA was performed using a thermogravimetric analyzer (PerkinElmer TGA 4000). The scan was conducted in a nitrogen atmosphere with a ramp rate of 20 ^{o}C min 1 and a scanning temperature range

of 30 ^{o}C to 800 ^{o}C. Approximately 5 mg of oven-dried sample was placed in an alumina crucible for testing.

2.12. Differential Scanning Calorimetry (DSC)

The DSC of the samples was performed with a PerkinElmer DSC 8000. Each sample (~ 6 mg) was weighed into a standard aluminum pan (40 µL) and heated under a nitrogen atmosphere with a flow rate of 15 mL min^{-1}. The sample was heated to 250°C at a rate of 10°C min^{-1}.

2.13. Rheological properties

The rheological properties of the SA-lignin hydrogel were measured using an MCR-101 Rheometer (Anton Paar, Japan). A freshly prepared SA-lignin hydrogel was utilized to record the rheological data at room temperature (25 ^{o}C). Both frequency sweep and amplitude sweep were run to determine the viscoelastic nature of the SA-lignin hydrogel. A space of 0.5 mm was maintained between the plate and samples during the experiments.

2.14. Scanning electron microscope (SEM)

The surface morphology of the lignin, lignin hydrogel, SA-lignin hydrogel, TSP fertilizer, TSP-loaded SA-lignin hydrogel, and TSP-coated fertilizer samples was determined using a scanning electron microscope (SEM) (JSM-IT300LV, Japan). All samples were dried for 12 h in a hot air oven at 50 ^{o}C. The samples were coated with a gold sputter coater, JEC 300. The SEM chamber was under a base pressure of 10^{-7} Torr.

2.15. Swelling capacity

To measure the swelling capacity of the hydrogel, 1 g of dry hydrogel was submerged in DI water for 24 h. Then the swollen hydrogel was removed from water, and surface water was removed by using filter paper and weighed. The swelling capacity of the hydrogel was calculated by the following equation [16].

$$Swelling\ capacity\ (\%) = \frac{S_s - S_d}{S_d} \times 100\,\% \ldots\ldots\ldots\ldots\ldots\ldots\ldots\ldots\ldots\ldots (2)$$

Where, S_s and S_d denote the weights of the swollen hydrogel sample and the dry hydrogel sample, respectively.

2.16. Water retention in soil/hydrogel mixture

The water retention of the soil/hydrogel mixture was determined to analyze the suitability of the hydrogels for agricultural applications. A dry hydrogel of 5 g was mixed with 100 g of dry soil and placed in a pot. A control soil sample without hydrogel was prepared. Then 100 mL of water was given to the pots. All experimental setups were incubated to maintain the same environmental conditions. The weights of the pots were recorded daily and continued until no further change in weights was observed. The water retention of the soil/hydrogel mixture was determined by the equation [17].

$$Water\ retention\ (\%) = \frac{W_t}{W_o} \times 100\ \%$$

3

where, W_t is the weight of water present in the soil at a time, t, and W_o is the initial weight of water in the soil.

2.17. Maximum water holding capacity (MWHC)

To measure the MWHC, 5 g of dry hydrogel was mixed with 100 g of dry soil and kept in a container. The container had a hole at the bottom, and a filter was placed over the hole to prevent soil loss. A similar procedure was followed for preparing all samples. All the containers were placed beneath the water tap and allowed to fill with water, ensuring maximum water absorption. After maximum water absorption, the containers were removed from the water tap and left to dry in the air for 2 hours to remove excess water. The water absorption of the soil was calculated by the following equation [14].

MWHC = Weight of [(Wet soil – Dry soil) – (Wet filter paper)] ..... (4)

2.18. Biodegradability assessment

The weight loss of SA-lignin hydrogel was assessed by soil burial method with incubation of hydrogel (1.0 g) for 90 days in light-texture sandy loam soil. The hydrogel sample was buried at a depth of ~ 8 cm from the topsoil and watered with 20 mL of DI water every five days and incubated at ~ 25 ^{o}C. After each interval of 30 days, the hydrogel samples were retrieved and cleaned with DI water and dried in oven at 60 ^{o}C. The weight loss was calculated using the following equation [18].

$$Weight\ loss\ (\%) = \frac{M_i - M_f}{M_i} \times 100\ \% \ldots\ldots\ldots\ldots\ldots\ldots\ldots\ldots\ldots\ldots (5)$$

Where, M_i and M_f denote the initial and final weights of the dried hydrogel samples.

2.19. Phosphorous release study

The release of phosphorus from TSP-loaded SA-lignin hydrogel and TSP-coated fertilizer was measured by a UV-Visible spectrophotometer. A dry weight of TSP-loaded SA-lignin hydrogel or TSP-coated fertilizer (1.0 g) was placed in a beaker containing 25 mL DI water under unstirred conditions. Then, 1 mL of the phosphorus-containing solution was withdrawn at a fixed time interval. To maintain a steady volume, an equal amount of 1 mL of DI water was added to the beaker. The sample was diluted, and the phosphorus was determined using ammonium-molybdate and phenol colorimetric methods [19]. A calibration curve was drawn using standards. At different time intervals, the absorbance of the release medium was measured and compared to the standard calibration curve, allowing for the determination of phosphorus release.

The phosphorus leaching experiment in soil was performed by collecting soil from the farm land of Delhi Technological University, Delhi. The pH and electrical conductivity of the soil samples were 8.5 and 0.95 μS/cm, respectively. The soil was light-texture sandy loam. The available phosphorus content present in the soil ~ 31 ppm. A fixed amount (1 g) of TSP-loaded SA-lignin hydrogel or TSP-coated fertilizer was mixed with dry soil (200 g) and placed into a leaching container. Then, 50 mL of DI water was poured into the mixture. The leaching was sampled by opening the valve. The weight of the leaching container was kept constant by adding DI water periodically. The amount of phosphorus was determined by the above-mentioned ammonium-molybdate and phenol colorimetric methods. All experiments were performed at room temperature (~ 25 ^{o}C).

2.20. Statistical Analysis

The data were presented as mean ± standard deviation of triplicate experiments. Microsoft Excel 2025 and Origin 2025 were used for data processing. The differences were considered significant at $p < 0.05$. F- values were calculated for the assessment of the relative variation between and within groups. The comparisons between two group were performed using a t-test. Significance levels are marked as $p < 0.05$ (*), $p < 0.01$ (**), and $p < 0.001$ (***).

3. Results and discussion

3.1. Phenolic hydroxyl group content in lignin and hydrogel sample

Lignin was extracted and isolated from mustard straw by the alkaline method. The yield of lignin by hot air oven drying was determined to be ~ 20.5%. The total phenolic hydroxyl group content in lignin was observed to be 2.215 mmol/g, which corresponds to the reported value [20]. The amounts of phenolic hydroxyl groups in lignin hydrogel, SA-lignin hydrogel, and TSP-SA-lignin hydrogel were determined to be 1.792 mmol/g, 1.526 mmol/g, and 1.356 mmol/g, respectively. The chemical reaction occurs when a hydrogel or composite is formed through cross-linking, resulting in the consumption of hydroxyl groups. The SA-lignin hydrogel utilizes the functional groups of lignin and SA to form cross-links, thereby reducing the total phenolic hydroxyl group content.

3.2. Fourier Transform Infrared Spectroscopy (FTIR)

The FTIR spectra of lignin, lignin hydrogel, SA-lignin hydrogel, and TSP-SA-lignin hydrogel are shown in Fig. 2a. The bands at 700, 804, 863, 877, 927, 946, 1035, and 1053 cm^{-1}, corresponding to C-O, and C-O-C stretching vibration in ester groups, C-O deformation in secondary alcohol and aliphatic ethers, and C-H deformation vibration. The bands at 1415 and 1455 cm^{-1} are attributed to the C-H bending from methyl or methylene groups and the C-H asymmetric deformation of the methyl group [21]. The transmutation of the C = O (carboxylic acid and aldehyde groups) band in lignin and lignin hydrogel appeared at 1639 cm^{-1} and 1637 cm^{-1}, respectively [22]. The bands at 2861, 2875 cm^{-1}, and 2933 cm^{-}

^{1} are attributed to the C-H (CH_3, CH_2, and CH) stretching vibration of the aliphatic groups of lignin hydrogel. A broad band of -OH in lignin hydrogel, characterized by an H-bond, appears at 3343 cm^{-1}, whereas in lignin, it is observed at 3345 cm^{-1} [23].

The TSP exhibits the characteristic frequency bands of Ca-O bonds, observed at 563, 656, and 851 cm^{-1}. The fundamental vibrational modes of the $[H_2PO_4]^-$ ion include the bending of O – P–O, the P – O stretching, in-plane P-O-H, and out-of-plane P – O–H, which are observed in the region of 500–600, 900–1100,1200–1250, and 800–900 cm^{-1}, respectively [24]. The TSP-SA-lignin hydrogel exhibits characteristic frequency bands at 854, 928, and 1051 cm^{-1}, corresponding to the Ca-O bond, the O – P–O, and P – O stretching frequencies, respectively. Therefore, TSP is properly loaded into the SA-lignin hydrogel.

3.3. Thermogravimetric analysis (TGA)

The TGA of lignin, lignin hydrogel, SA-lignin hydrogel, and TSP-SA-lignin hydrogel was studied, showing distinct zones of weight loss as depicted in Fig. 2b. TGA plots showed the thermal stability and thermal properties of polymers and hydrogels. The first weight loss of the polymer and hydrogel was due to the removal of moisture, and the second weight loss could be attributed to the degradation of -OH and -COOH groups in the polymers and hydrogels. Third and fourth weight loss could be attributed to the degradation of the backbone of polymers and hydrogels. The total weight loss of lignin, lignin hydrogel, SA-lignin hydrogel, and TSP-SA-lignin hydrogel was 60.83%, 56.67%, 27.61%, and 23.85% respectively, at 900 ^{o}C, showing less weight loss of TSP-SA-lignin hydrogel due to the presence of inorganic salt (TSP). The interaction between TSP and lignin/sodium alginate results in a more thermally stable material. However, TGA of SA was reported showing the sharp decomposition peak at 242 ^{o}C [25]. Another reported TGA of SA elucidated the initial weight loss of 11.27% at 30–125 ^{o}C and second step weight loss of ~ 33.98% in the range of 125–250 ^{o}C [26]. Based on thermal studies, it is clear that our synthesized hydrogel and fabricated fertilizer are thermally stable. The thermal stability of hydrogels and in-situ-loaded or coated fertilizers is an important parameter, as it influences the quality, safety, and farming efficiency of the materials. The physical or chemical decomposition of the hydrogels and fertilizers may be influenced by temperature. The hydrogels and fertilizers retain their chemical composition intact and remain effective by maintaining their thermal stability. So, the thermal instability can affect the physical properties of fertilizer granules, complicating field application.

3.4. Differential Scanning Calorimetry (DSC)

The DSC of lignin, lignin hydrogel, SA-lignin hydrogel, and TSP-SA-lignin hydrogel was performed as shown in Fig. 2c. The glass transition temperatures (Tg) of the polymer and hydrogel were determined, which are essential characteristics of polymers and hydrogels for their applicability. The lignin hydrogel exhibited a higher Tg value of 115 ^{o}C compared to lignin, which had an observed Tg value of 110 ^{o}C due to crosslinking in lignin and ECH. It was reported that SA showed the first endothermic peak at ~ 100 ^{o}C and second exothermic peak at ~ 250 ^{o}C, which may be attributed to the moisture release and

decomposition, respectively, of the SA [27]. However, the Tg of SA-lignin hydrogel increases due to the crosslinking and hydrogen bonding between SA and lignin. The combination of SA and lignin creates a more densely cross-linked network, and these cross-links restrict the polymer composite chains, requiring more energy to move and thus enhancing the Tg. SA also increases the composite's rigidity and elevates the temperature at which it transitions from a rigid, glassy state to a softer, rubbery state. That's why the Tg of SA-lignin is higher than that of lignin and lignin hydrogel. The Tg of SA-lignin hydrogel was determined as 160 ^{o}C. When TSP was loaded into SA-lignin hydrogel, the Tg value decreased due to plasticizing effect, intermolecular interactions, and moisture absorption. The inorganic TSP acts as a filler and plasticizer in the polymer matrix. In the presence of TSP in SA-lignin, it enhances the moisture content for hydrophilic SA, thus leading to a lower Tg [28]. However, the TSP-loaded SA-lignin hydrogel showed the dehydration evidenced by an endothermic peak at ~ 100 ^{o}C, then the decomposition takes place by an exothermic peak at ~ 200 ^{o}C [27]. As the SA-lignin hydrogel possesses the highest Tg, it indicates that the SA-lignin hydrogel is rigid and glassy at higher temperatures. On the other hand, lignin possessed a lower Tg compared to lignin hydrogel and SA-lignin hydrogel, suggesting it is softer and rubbery at lower temperatures.

3.5. Rheological Properties

The amplitude sweep in rheology was performed (Fig. 3a) to characterize the viscoelastic properties of the SA-lignin hydrogel, to determine the relationship between shear strain and shear stress, and to identify the linear viscoelastic (LVE) region and the yield point, or flow point, or crossover point. The internal structure of the SA-lignin hydrogel is undisturbed in the LVE region at low shear strains. In this LVE region, shear stress is directly proportional to the shear strain, i.e., the ratio of shear stress and shear strain provides a constant modulus, and storage modulus (G') and loss modulus (G") remain constant, independent of the applied strain or stress amplitude [29]. The LVE region for SA-lignin hydrogel was determined as 0.0001% to 0.18% of shear strain. The G' (~ 147 Pa) is higher than G" (~ 28 Pa), and both moduli decrease with the enhancement of shear strain or shear stress, and the moduli begin to drop. The drop of the modulus also marks the limit of the LVE region, which is known as the yield point [30]. The yield point of the SA-lignin hydrogel was determined as 0.17% of shear strain. After falling down the moduli, G' crossovers G", and a crossover point is created, called the flow point or crossover point. The crossover point of the SA-lignin hydrogel is determined to be 1% shear strain. After the crossover point, viscous behavior begins to dominate, and the polymer starts to flow like a liquid [31].

To characterize the viscoelastic properties of the SA-lignin hydrogel, an angular frequency sweep in rheology was performed, as shown in Fig. 3b. The storage modulus (G') and loss modulus (G") of the SA-lignin hydrogel increase with increasing angular frequency. The polymer is probed at shorter time scales at higher frequencies, and the molecular structural elements or chains have less time to relax and flow, thus exhibiting more solid-like behavior [32]. The SA-lignin hydrogel exhibits permanently elastic behavior across the frequency range of 0.1 rad/s to 100 rad/s, as G' (~ 100 Pa) is consistently higher than G" (~ 40 Pa). Therefore, the SA-lignin hydrogel is solid-like and elastic, storing more energy than it dissipates.

No crossover is observed in the frequency range of 0.1 rad/s to 100 rad/s, confirming the SA-lignin hydrogel has a solid-like nature across the measured frequency range.

The mechanical properties of the SA-lignin hydrogel were analyzed with shear stress and shear strain, as shown in Fig. 3c. The linear elastic region of the curve gives the value of Young's modulus, which is determined for SA-lignin hydrogel as 0.946 Pa. Young's modulus, also known as the elastic modulus, indicates the stiffness or resistance to elastic (reversible) deformation under tensile or compressive stress [33]. From the curve, tensile strength was determined to be ~ 88 Pa, indicating the maximum stress that the SA-lignin hydrogel can withstand before it begins to break under tension [34]. The breakpoint, also known as the fracture point, is the point on the curve where the SA-lignin hydrogel breaks. The breakpoint of the SA-lignin hydrogel was determined to be 10% shear strain. Based on the rheological properties of the SA-lignin hydrogel, it can be used as a water reservoir, a soil conditioner, and a controlled-release carrier for nutrients or pesticides in a real-world soil environment [4].

3.6. Morphology of biopolymer and hydrogel

The SEM images of the lignin, lignin hydrogel, and SA-lignin hydrogel are shown in Fig. 4. Lignin appears heterogeneous with a sand-slag-like compound and various sizes of rough balls. The diameters of the rough balls were observed in the range of 11 to 15 μm (Fig. 4a). Lignin hydrogel shows an interlinked porous surface. The pores are very complex and create a sponge-like three-dimensional structure (Fig. 4b). However, SA-lignin hydrogel exhibits a three-dimensional cross-linked network, in which lignin provides the structural integrity and SA provides the necessary structure to more closely mimic the native extracellular matrix [35]. The wrinkled morphology of SA-lignin hydrogel also exhibits a porous texture with an irregular surface (Fig. 4c). The morphology of pure SA was reported as smooth, flat, and compact [36]. But when SA is mixed with lignin, lignin serves as a flexible skeleton, and SA is crosslinked around the lignin skeleton [35].

3.7. Swelling capacity and water retention

The swelling capacity of lignin hydrogel, SA-lignin hydrogel, TSP-loaded SA-lignin hydrogel, and TSP-coated fertilizer was studied in DI water, as depicted in Fig. 5a. The SA-lignin hydrogel exhibited the highest swelling capacity due to its larger pores and cavities, allowing the polymeric network to expand more freely. When the TSP was introduced into the SA-lignin mixture, the swelling capacity of the TSP-SA-lignin hydrogel decreased due to the formation of a compact network. TSP provides calcium ions, which create ionic crosslinks between TSP and SA-lignin, forming a more rigid, compact network and thus restricting the swelling capacity. The calcium ions interact with the carboxylate groups of alginates, creating a strong ionic cross-linked structure of calcium alginate. TSP-coated fertilizers were prepared by encapsulating TSP with SA-lignin hydrogel. The TSP-coated fertilizer showed lower swelling capacity compared to the TSP-loaded SA-lignin hydrogel. TSP-loaded SA-lignin hydrogel was prepared by the in-situ method, where a smaller quantity of TSP was blended into the SA-lignin mixture. Less TSP results in

fewer calcium ions, so the ionic interaction between TSP and SA-lignin is less in TSP-loaded SA-lignin hydrogel, resulting in more swelling compared to TSP-coated fertilizer.

The water retention of lignin hydrogel, SA-lignin hydrogel, TSP-loaded SA-lignin hydrogel, and TSP-coated fertilizer was also evaluated in a soil/hydrogel mixture as depicted in Fig. 5b. The soil/SA-lignin hydrogel mixture retained more water and took longer to dry due to the non-rigid network of the SA-lignin hydrogel. The control soil was dried earlier compared to the soil/hydrogel mixture, so the hydrogel facilitates the soil in retaining water over an extended period. The soil/SA-lignin hydrogel mixture retained water for ~ 50 days longer compared to the control soil. It was reported that rice straw cellulose blended with carboxymethyl tamarind kernel gum exhibited water absorption capacity in the range of 663–832% in DI water [37].

The maximum water holding capacity of soil was also evaluated in the presence of lignin hydrogel, SA-lignin hydrogel, TSP-loaded SA-lignin hydrogel, and TSP-coated fertilizer (Fig. 5c). The soil-incorporated hydrogel showed greater water retention compared to the control soil. The MWHC of soil incorporated lignin hydrogel, SA-lignin hydrogel, TSP-loaded SA-lignin hydrogel, and TSP-coated fertilizer exhibited 37 g, 55 g, 43 g, and 39 g of water, whereas the control soil showed 25 g of water.

3.8. Biodegradability assessment

The weight loss method is one of the effective ways to assess the biodegradation performance of hydrogel in the soil. The weight loss of the hydrogel under different burial time is shown in Fig. 5d. With the enhancement of burial time, the biodegradation of the hydrogel samples in the soil gradually increases. The weight loss of the hydrogel samples after 30, 60, and 90 days were 41.87%, 53.25% and 77.37%, respectively. The weight loss of lignin hydrogel was reported 17.26% after 60 days of incubation [18]. The biodegradation study of lignin-chitosan hydrogel was reported 67.68% of weight loss after 60 days of soil burial [4].

3.9. Morphological and physicochemical properties of TSP-loaded SA-lignin hydrogel

The TSP pellet was viewed using the SEM, as shown in Fig. 6a. The pellet was selected randomly, and its powdered form was also scanned, revealing a very rough, unsmooth surface (Fig. 6b). The TSP fertilizer was powdered and loaded into SA-lignin hydrogel using the in-situ method. The TSP-loaded SA-lignin hydrogel was observed using SEM. The SEM images showcase the convoluted porous surface (Fig. 6c, and d). Many porous pellets with various shapes and sizes were formed. The calcium ions in TSP form a bond with SA through ionic crosslinking. The sodium ions in SA are replaced by calcium ions, which bind to the carboxylate groups on the alginate chains. Lignin interacts with SA through its various functional groups (e.g., carboxylic and phenolic groups), forming a SA-lignin composite matrix. This SA-lignin composite matrix can be incorporated by TSP into the calcium alginate network.

3.10. Morphological and physicochemical properties of coated TSP fertilizers

TSP granules were coated using SA-lignin hydrogel. After coating, the TSP granules gained ~ 2% weight. The morphology of the coated TSP fertilizers was analyzed by SEM and depicted in Fig. 7. A granule from TSP-coated fertilizers was randomly selected and cut in half using scissors. The thickness of the coating layer was evaluated by using the drawing rule option of the SEM.

The TSP granules were successfully coated with SA-lignin hydrogel. The visual aspect of coated TSP fertilizers was nearly identical to that of uncoated TSP fertilizer. The coated TSP fertilizers were a yellowish-brown color, while the uncoated TSP fertilizers were gray. The cross-sectional SEM images of the coated TSP clearly showed the coating and the fertilizer. The coating, SA-lignin hydrogel film, exhibited a porous, and irregular structure. The adhesion and border between the coating and TSP were difficult to differentiate due to the rough surface of both the TSP and the coating. The thickness of the coating on coated TSP fertilizers was determined, resulting in a range of 402 to 758 μm. The thickness of the coating influences the slow and controlled release of nutrients. It was reported that low thickness increased the release rate of phosphorus, showing that coated pellets with a thickness of 63 μm released 325 g P/m³, while those with a thickness of 128 μm released 225 g P/m³ within 10 days [38]. Therefore, the release rate can be controlled by adjusting the thickness of the coating polymer.

3.11. EDX study of TSP, TSP-loaded SA-lignin hydrogel, and TSP-coated fertilizer

The elemental compositions (wt.%) of TSP fertilizer, TSP-loaded SA-lignin hydrogel, and TSP-coated fertilizer were analyzed with EDX, as shown in Fig. 7. The EDX graph reveals that TSP is composed of phosphorus (23.3%), calcium (10.4%), and oxygen (61.7%), as well as some trace elements (Fig. 7g). The TSP-loaded SA-lignin hydrogel reveals its elemental composition (wt.%) as mainly phosphorus (21.3%), sodium (15.9%), calcium (10.7%), and oxygen (50.9%), with trace amounts of other elements (Fig. 7h). However, the TSP-coated fertilizer primarily consists of phosphorus (18.6%), sodium (7.6%), calcium (12.9%), and oxygen (53.8%), with a trivial amount of other elements (Fig. 7i). The wt.% of TSP-loaded SA-lignin hydrogel and TSP-coated fertilizer varies slightly due to the variation of interactions between the TSP and SA-lignin hydrogel. In the TSP-loaded SA-lignin hydrogel, TSP was added to the SA-lignin mixture, and then the TSP-loaded hydrogel was prepared by the in-situ technique. On the other hand, the TSP-coated fertilizer was prepared by coating the TSP fertilizer with SA-lignin hydrogel. Therefore, the interactions between TSP and SA-lignin differ in TSP-loaded SA-lignin hydrogel and TSP-coated fertilizer, resulting in variations in wt.% composition. It is noted that SEM-EDX is a surface-sensitive and semi-quantitative technique. From EDX, we only analyzed the elemental composition of surface of the samples.

3.12. Slow release of phosphorus from TSP-loaded SA-lignin hydrogel

The release of phosphorus from TSP-loaded SA-lignin hydrogel exhibited a fractional release of 0.92, i.e., the cumulative release was 92% after 20 days in DI water (Fig. 8a). A similar study was reported, illustrating that the cumulative release of phosphorus from SA/calcium-modified montmorillonite/lignin composite was ~ 24% after 3 days in water [9]. It is reported that pure TSP releases 100% phosphorus within 24 h in water [39]. Therefore, the TSP-loaded SA-lignin hydrogel is more effective for the slow release of phosphorus compared to pure TSP.

Table 2
The kinetic parameters of P release from TSP-loaded SA-lignin hydrogel samples in DI water and soil

Kinetic models	Parameter	DI water	Soil
Korsmeyer-Peppas	R^2	0.777	0.961
$\frac{M_t}{M_\infty} = K_{KP}t^n$	n	0.366	0.588
	K_{KP}	0.343	0.095
Higuchi	R^2	0.721	0.953
$\frac{M_t}{M_\infty} = K_H t^{1/2}$	K_H	0.241	0.128
Peppas-Shalin	R^2	0.938	0.994
$\frac{M_t}{M_\infty} = k_1 t^m + k_2 t^{2m}$	m	0.795	0.929
	k_1	0.239	0.059
	k_2	-0.015	-0.001
Zero-order	R^2	0.043	0.879
$\frac{M_t}{M_\infty} = K_0 t$	K_o	0.059	0.022
First-order	R^2	0.938	0.979
$\frac{M_t}{M_\infty} = 1 - e^{-K_1 t}$	K_1	0.236	0.046

The release fraction of phosphorus was fitted into standard empirical kinetic models to analyze the release data. The Korsmeyer-Peppas model, Higuchi model, Peppas-Sahlin model, zero-order model, and first-order model were used to determine the release parameters and mechanisms (Table 2). In the expression shown in Table 2, $\frac{M_t}{M_\infty}$ is the amount of release fraction released at time t, K_{KP} is the release

rate constant, and *n* is the release exponent. K_H is the Higuchi dissolution constant. k_1 and k_2 are diffusional constants related to Fickian and non-Fickian mechanism contributions. m is the diffusion coefficient. K_0 is the zero-order rate constant, and K_1 is the first-order rate constant.

The correlation coefficients (R^2) are determined for each phosphorus release profile against each model listed in Table 2, and the best-fit model is used to evaluate the possible mechanism of phosphorus release. The release profile showed that the release of phosphorus in DI water from TSP-loaded SA-lignin hydrogel is governed by the Peppas-Shalin model (R^2 = 0.938) and the first-order model (R^2 = 0.938). The Peppas-Shalin model exhibits Fickian diffusion, accompanied by polymer relaxation from a swellable matrix. The diffusional exponent (m = 0.795) suggests the release mechanism as Fickian diffusion and polymer relaxation. However, the magnitude of the release constant k_1 (0.239) is greater than k_2 (0.015), indicating that phosphorus release from SA-lignin hydrogel is mainly Fickian diffusion-controlled rather than relaxation-controlled. Therefore, the release of phosphorus from SA-lignin hydrogel in DI water is dominated by diffusion rather than relaxation.

The cumulative release of phosphorus from TSP-loaded SA-lignin hydrogel samples in soil is shown in Fig. 8b, revealing a gradual release of phosphorus over time, reaching 77% in 40 days. A similar study was reported, demonstrating that the cumulative release of nitrogen and phosphorus from SA/sanxan/lignin was 77.08% and 68.71% respectively, in soil on the 28th day [40].

The release data (Table 2) indicate that the Peppas-Sahlin model (Fig. 8b) is the best-fit model, as evidenced by the high correlation coefficient (R^2 = 0.99), which approaches 1. The diffusional exponent (m = 0.929) indicates that phosphorus release from SA-lignin hydrogel in soil is regulated by diffusion and relaxation with swelling. The release constant, k_1 (0.059), is greater than k_2 (0.001), indicating that diffusion is more prominent than relaxation. These findings suggest that TSP fertilizer molecules are distributed uniformly in the SA-lignin hydrogel and the release is primarily controlled by diffusion rather than relaxation, degradation, or erosion.

3.13. Slow release of phosphorus from coated TSP fertilizer

The encapsulation of TSP in the SA-lignin hydrogel for the slow release of phosphorus is studied using empirical kinetic models. The amount of phosphorus released from coated TSP fertilizer is determined, showing the cumulative release of 95% in DI water after 10 days (Fig. 8c). A similar cumulative release of urea was reported, demonstrating a 51% release from coated urea (coated with a lignin-polybutylene adipate-co-terephthalate-starch bilayer nanohybrid bio-composite) in water after 5 days [41].

Table 3
The kinetic parameters of P release from TSP-coated fertilizer samples in DI water, and soil

Kinetic models	Parameter	DI water	Soil
Korsmeyer-Peppas	R^2	0.937	0.979
	n	0.785	0.738
	K_{KP}	0.176	0.096
Higuchi	R^2	0.872	0.921
	K_H	0.303	0.179
Peppas-Shalin	R^2	0.995	0.997
	m	0.005	0.996
	k_1	0.631	0.079
	k_2	-0.632	-0.002
Zero-order	R^2	0.923	0.952
	K_o	0.112	0.045
First-order	R^2	0.959	0.994
	K_1	0.268	0.094

The kinetic models reveal that the Peppas-Sahlin model is the best-fit model, as the correlation coefficient R^2 (= 0.99) is equivalent to 1. The diffusional exponent (m = 0.005) indicates that the release is controlled by diffusion (Table 3). But the kinetic constants express the equal contribution of diffusion and relaxation. The magnitude of the kinetic constants, k_1 (0.631) and k_2 (0.632), is equivalent. Therefore, the release of phosphorus from TSP-coated fertilizer in DI water is governed by both diffusion and polymer relaxation, accompanied by swelling.

The release of phosphorus from coated TSP fertilizer is determined, with 88% of the phosphorus released into the soil after 22 days (Fig. 8d). A similar report showed that the release of phosphorus from coated DAP was 30.03% after 30 days of incubation in soil, when it was covered by hydroxyethyl cellulose [19]. Kinetic parameters show that the Peppas-Sahlin model is the best fit model (R^2 = 0.99). The diffusional exponent (m = 0.996) demonstrates both diffusion and relaxation. However, the release constant, k_1 (0.079), is predominant over k_2 (0.002), indicating that diffusion is more pronounced than relaxation.

The phosphorus release in water from in-situ loading hydrogel and coated fertilizer follows the Peppas-Sahlin model. The in-situ loaded hydrogel (m = 0.795) showed a larger diffusional exponent than the coated fertilizer (m = 0.005), indicating that the in-situ loaded hydrogel follows Fickian diffusion as well as relaxation. In contrast, the coated fertilizer follows merely Fickian diffusion. The in-situ loaded hydrogel showed lower release constants (k_1 = 0.239; k_2 = -0.015) than those of the coated fertilizer (k_1 = 0.631; k_2 = -0.632), indicating that the coated fertilizer releases phosphorus faster in water.

The phosphorus release from in-situ loading hydrogel and coated fertilizer in soil follows the Peppas-Sahlin model—both the in-situ-loaded hydrogel and the coated fertilizer exhibit Fickian diffusion with relaxation. But the coated fertilizer (m = 0.996) exhibited more Fickian diffusion with relaxation than the in-situ-loaded hydrogel (m = 0.929). The coated fertilizer (k_1 = 0.079; k_2 = -0.002) showed higher release constants than those of the in-situ loaded hydrogel (k_1 = 0.059; k_2 = -0.001), indicating that the coated fertilizer exhibits faster phosphorus release in soil.

4. Conclusion

The sustained release of nutrients in agriculture has altered conventional fertilization practices by enhancing the utilization of fertilizer through the control of leaching. Conventional fertilization is ineffective in controlling leaching and contributes to environmental pollution. To address these challenges, we have proposed a sustainable and practical approach to upcycle agricultural waste, mustard straw, into a lignin-based hydrogel for use as a carrier of triple superphosphate (TSP) fertilizer. The primary objective of this study was to upcycle agricultural waste into a biomass-based hydrogel for farming applications, including water retention and the slow and controlled release of fertilizer. The swelling capacities of lignin hydrogel, SA-lignin hydrogel, TSP-loaded SA-lignin hydrogel, and TSP-coated fertilizer were 305%, 3702%, 2506%, and 2058%, respectively, in DI water. The soil/SA-lignin hydrogel mixture retained water for ~ 50 days longer compared to the control soil. The MWHC of soil incorporated lignin hydrogel, SA-lignin hydrogel, TSP-loaded SA-lignin hydrogel, and TSP-coated fertilizer exhibited 37 g, 55 g, 43 g, and 39 g of water, whereas the control soil showed 25 g of water. We have utilized the SA-lignin hydrogel as a carrier of TSP in two different ways. Firstly, TSP was loaded into SA-lignin hydrogel using the in-situ technique, and the release was monitored using empirical kinetic models. The results showed that the Peppas-Sahlin model was the best-fit model, indicating that the release is governed primarily by diffusion rather than relaxation or polymer swelling. Secondly, TSP was coated with SA-lignin hydrogel, and the release profiles were evaluated using kinetic models, showing that the Peppas-Sahlin model was the best-fit model, indicating that the release is controlled by both diffusion and relaxation, or polymer swelling. However, the cumulative release of phosphorus from TSP-loaded SA-lignin hydrogel samples showed 92% after 20 days in DI water and 77% after 40 days in soil. On the other hand, TSP-coated fertilizer showed a cumulative release of phosphorus 95% after 10 days in DI water and 88% after 22 days in soil. Moreover, pure TSP releases 100% phosphorus within 24 h. Therefore, the entrapment and encapsulation of TSP by SA-lignin hydrogel is more convenient for the slow release of phosphorus compared to pure TSP. In our approach, all types of fertilizer granules, including monoammonium

phosphate (MAP), diammonium phosphate (DAP), urea, and, nitrogen, phosphorus and potassium fertilizer (NPK fertilizer) can be properly entrapped and encapsulated. These findings suggest that our prepared SA-lignin hydrogel has the potential to be applied in farming practices for sustainable production.

Declarations

Declaration of competing interest

The authors declare that they have no known competing financial interests or personal relationships that could have appeared to influence the work reported in this paper.

Funding

Not applicable

Author Contribution

Tarun Kumar Gayen: Conceptualization, Data curation, Formal analysis, Investigation, Methodology, Project administration, Resources, Software, Validation, Visualisation, Writing - original draft, Writing - review & editing. Mohammad Amdad Ali: Supervision, Writing - review & editing. Sudhir G Warkar: Supervision, Writing - review & editing.

Acknowledgement

N/A

Data availability

Data will be made available on request.

References

1. Alonso-Cuevas CF, Ramírez-Guzmán N, Serna-Cock L et al (2025) From Agro-Industrial Waste to Natural Hydrogels: A Sustainable Alternative to Reduce Water Use in Agriculture. Gels 11:616. https://doi.org/10.3390/gels11080616
2. Basak A, Mahanty AK, Ghosh S (2025) Enzymatic synergy in lignocellulase cocktail of a thermotolerant bacterial consortium enhances rice straw saccharification. Biomass Convers

Biorefin. https://doi.org/10.1007/s13399-025-06658-7

3. Manna D, Chowdhury R, Kuittinen S et al (2025) Environmental sustainability assessment of mustard straw torrefaction: Insights from thermo-kinetics, product distribution analysis, product characterization and life cycle assessment. Biomass Bioenergy 201:108110. https://doi.org/10.1016/J.BIOMBIOE.2025.108110
4. Gayen TK, Ali MA, Warkar SG (2026) Agricultural Waste-Derived Lignin and Chitosan Blend Biohydrogels for Controlled Release of Muriate of Potash for Sustainable Agricultural Applications. Ind Eng Chem Res. https://doi.org/10.1021/acs.iecr.5c05055
5. Zhang YM, Zhao Q, Li L et al (2018) Synthesis of a lignin-based phosphorus-containing flame retardant and its application in polyurethane. RSC Adv 8:32252–32261. https://doi.org/10.1039/c8ra05598j
6. Liu X, Zhan J, Ren S et al (2025) Mechanically robust, recyclable lignin-reinforced photothermal shape memory polymers containing dynamic boronic ester bonds. Chem Eng J 523:168185. https://doi.org/10.1016/J.CEJ.2025.168185
7. Li H, Li Y, Yan H et al (2025) Preparation and slow-release property of modified lignin-coated sodium alginate fertilizer core double-layer coated fertilizer. J Polym Res 32. https://doi.org/10.1007/s10965-025-04594-8
8. Shojaeinia F, Haghbin Nazarpak M, Karkhaneh A (2025) Antioxidant and antibacterial alginate/lignin composite hydrogels loaded with vancomycin for wound dressing applications. J Biomater Appl 40:473–486. https://doi.org/10.1177/08853282251347768
9. Boussetta A, Ilsouk M, Lahcini M et al (2025) Synergistic effect of lignin and modified clay on alginate-based composites and their use in slow-release coating formulations for phosphorus fertilizers. Prog Org Coat. https://doi.org/10.1016/j.porgcoat.2024.109019. 200:
10. Li H, Li Y, Yan H et al (2025) Preparation and slow-release property of modified lignin-coated sodium alginate fertilizer core double-layer coated fertilizer. J Polym Res 32. https://doi.org/10.1007/s10965-025-04594-8
11. Sinha AK, Sharma MD, Mishra P, Kulshrestha S (2024) Food waste and sustainable development goals. Food Waste Valorization: Emerging Trends, Techno-economic and Environmental Considerations 19–31. https://doi.org/10.1016/B978-0-443-15958-9.00003-4
12. Almeida M, Vieira H (2025) Marine-Derived Collagen and Chitosan: Perspectives on Applications Using the Lens of UN SDGs and Blue Bioeconomy Strategies. Mar. Drugs 23
13. Daojie, Dong*, Arthur L, Fricke (1995) Intrinsic viscosity and the molecular weight of kraft lignin. Polym (Guildf) 36(10):2075–2078
14. Gayen TK, Ali MA, Warkar SG (2025) Cellulose Microfibers-Embedded Carboxymethyl Tamarind Kernel Gum Hydrogels as Soil Conditioners and Plant Nutrients Carriers. ACS Agricultural Sci Technol. https://doi.org/10.1021/acsagscitech.5c00092
15. Gärtner AGG and TTarja (1999) 1999 Determination of phenolic hydroxyl groups in residual lignin using a modified UV-method. Nord Pulp Paper Res J 14:163–170.

https://doi.org/https://doi.org/10.3183/npprj-1999-14-02-p163-170

16. Gayen TK, Ali MA, Warkar SG (2025) Carboxymethyl tamarind kernel gum bio-hydrogel for soil amendment and micronutrient release in sustainable agricultural technologies. Polym Bull. https://doi.org/10.1007/s00289-025-05995-x
17. Gayen TK, Ali MA, Warkar SG (2025) Synthesis of cellulose microfibrils embedded carboxymethyl tamarind kernel gum hydrogels for water retention and controlled urea release in agricultural applications. Int J Biol Macromol 319:145414. https://doi.org/10.1016/J.IJBIOMAC.2025.145414
18. Gayen TK, Warkar SG, Ali MA (2025) Valorization of Biomass-Derived Lignin into Hydrogels for Soil Hydration and Slow-Release Fertilization. Ind Eng Chem Res 64:23661–23671. https://doi.org/10.1021/acs.iecr.5c03927
19. El Bouchtaoui FZ, Ablouh EH, Mhada M et al (2024) Humic Acid-Functionalized Lignin-Based Coatings Regulate Nutrient Release and Promote Wheat Productivity and Grain Quality. ACS Appl Mater Interfaces 16:30355–30370. https://doi.org/10.1021/acsami.4c03224
20. Musl O, Sulaeva I, Sumerskii I et al (2021) Mapping of the Hydrophobic Composition of Lignosulfonates. ACS Sustain Chem Eng 9:16786–16795. https://doi.org/10.1021/acssuschemeng.1c06469
21. Sathawong S, Sridach W, Techato KA (2018) Lignin: Isolation and preparing the lignin based hydrogel. J Environ Chem Eng 6:5879–5888. https://doi.org/10.1016/J.JECE.2018.05.008
22. Mazloom N, Khorassani R, Zohuri GH et al (2019) Development and Characterization of Lignin-Based Hydrogel for Use in Agricultural Soils: Preliminary Evidence. Clean (Weinh) 47. https://doi.org/10.1002/clen.201900101
23. Saruchi KV, Ghfar AA, Pandey S (2023) Controlled release of harmful pesticide dichlorvos through synthesized biodegradable aloe vera–acrylic acid-based hydrogel and its utilization in soil water management. J Anal Sci Technol 14. https://doi.org/10.1186/s40543-023-00374-5
24. Seesanong S, Seangarun C, Boonchom B et al (2021) Composition and Properties of Triple Superphosphate Obtained from Oyster Shells and Various Concentrations of Phosphoric Acid. ACS Omega 6:22065–22072. https://doi.org/10.1021/acsomega.1c02660
25. Allaboun H, Fares MM, Abu Al-Rub FA (2016) Removal of uranium and associated contaminants from aqueous solutions using functional carbon nanotubes-sodium alginate conjugates. Minerals 6. https://doi.org/10.3390/min6010009
26. Salisu A, Sanagi MM, Abu Naim A et al (2016) Alginate graft polyacrylonitrile beads for the removal of lead from aqueous solutions. Polym Bull 73:519–537. https://doi.org/10.1007/s00289-015-1504-3
27. Soares JP, Santos JE, Chierice GO, Cavalheiro G (2004) ET Thermal behavior of alginic acid and its sodium salt
28. Sadeghi-Shapourabadi M, Robert M, Elkoun S (2025) A Study of the Influence of Sodium Alginate Molecular Weight and Its Crosslinking on the Properties of Potato Peel Waste-Based Films. Appl Sci (Switzerland) 15. https://doi.org/10.3390/app15126385

29. Ravishankar K, Venkatesan M, Desingh RP et al (2019) Biocompatible hydrogels of chitosan-alkali lignin for potential wound healing applications. Mater Sci Engineering: C 102:447–457. https://doi.org/10.1016/J.MSEC.2019.04.038
30. Zerpa A, Pakzad L, Fatehi P (2018) Hardwood Kraft Lignin-Based Hydrogels: Production and Performance. ACS Omega 3:8233–8242. https://doi.org/10.1021/acsomega.8b01176
31. Kratochvílová R, Kráčalík M, Smilková M et al (2023) Functional Hydrogels for Agricultural Application. https://doi.org/10.3390/gels9070590. Gels 9:
32. Chen J, Huang Y, Deng L et al (2023) Preparation and research of PCL/cellulose composites: Cellulose derived from agricultural wastes. Int J Biol Macromol 235:123785. https://doi.org/10.1016/J.IJBIOMAC.2023.123785
33. Cernekova N, Hricovini M, Vostrejs P, Kovalcik A (2025) Innovative antimicrobial lignins: Extraction and characterization for advanced hydrogel applications. Int J Biol Macromol 307:141959. https://doi.org/10.1016/J.IJBIOMAC.2025.141959
34. Ullah F, Khan MT, Shahzad A et al (2025) Fabrication of xanthan gum based polymeric hydrogels: Rheological investigation, toughness, and adhesion optimization. Int J Adhes Adhes 138:103955. https://doi.org/10.1016/J.IJADHADH.2025.103955
35. Shan Z, Jiang B, Wang P et al (2025) Sustainable lignin-based composite hydrogels for controlled drug release and self-healing in antimicrobial wound dressing. Int J Biol Macromol 285:138327. https://doi.org/10.1016/J.IJBIOMAC.2024.138327
36. Cheryl-Low YL, Theam KL, Lee HV (2015) Alginate-derived solid acid catalyst for esterification of low-cost palm fatty acid distillate. Energy Convers Manag 106:932–940. https://doi.org/10.1016/J.ENCONMAN.2015.10.018
37. Gayen TK, Warkar SG (2025) Micronutrient-Loaded Biopolymer as Slow-Release Behavior. IOCPS 2025. MDPI, Basel Switzerland, p 90
38. Ahmad NNR, Fernando WJN, Uzir MH (2015) Parametric evaluation using mechanistic model for release rate of phosphate ions from chitosan-coated phosphorus fertiliser pellets. Biosyst Eng 129:78–86. https://doi.org/10.1016/J.BIOSYSTEMSENG.2014.09.015
39. Rotondo F, Coniglio R, Cantera L et al (2018) Lignin-based coatings for controlled P-release fertilizer consisting of granulated simple superphosphate. Holzforschung 72:637–643. https://doi.org/10.1515/hf-2017-0176
40. He C, Huang Y, Shao Q et al (2025) Lignin-based ternary composite hydrogel for slow-release of fertilizer and soil water retention. Int J Biol Macromol 296:139679. https://doi.org/10.1016/J.IJBIOMAC.2025.139679
41. Bo W, Zhi-Peng L, Yue L et al (2025) Lignin-polybutylene adipate-co-terephthalate(PBAT)-starch@urea bilayer nanohybrid biocomposite enable superior controlled slow-released fertilizer with good water-retention. Int J Biol Macromol 310. https://doi.org/10.1016/j.ijbiomac.2025.142890

Figures

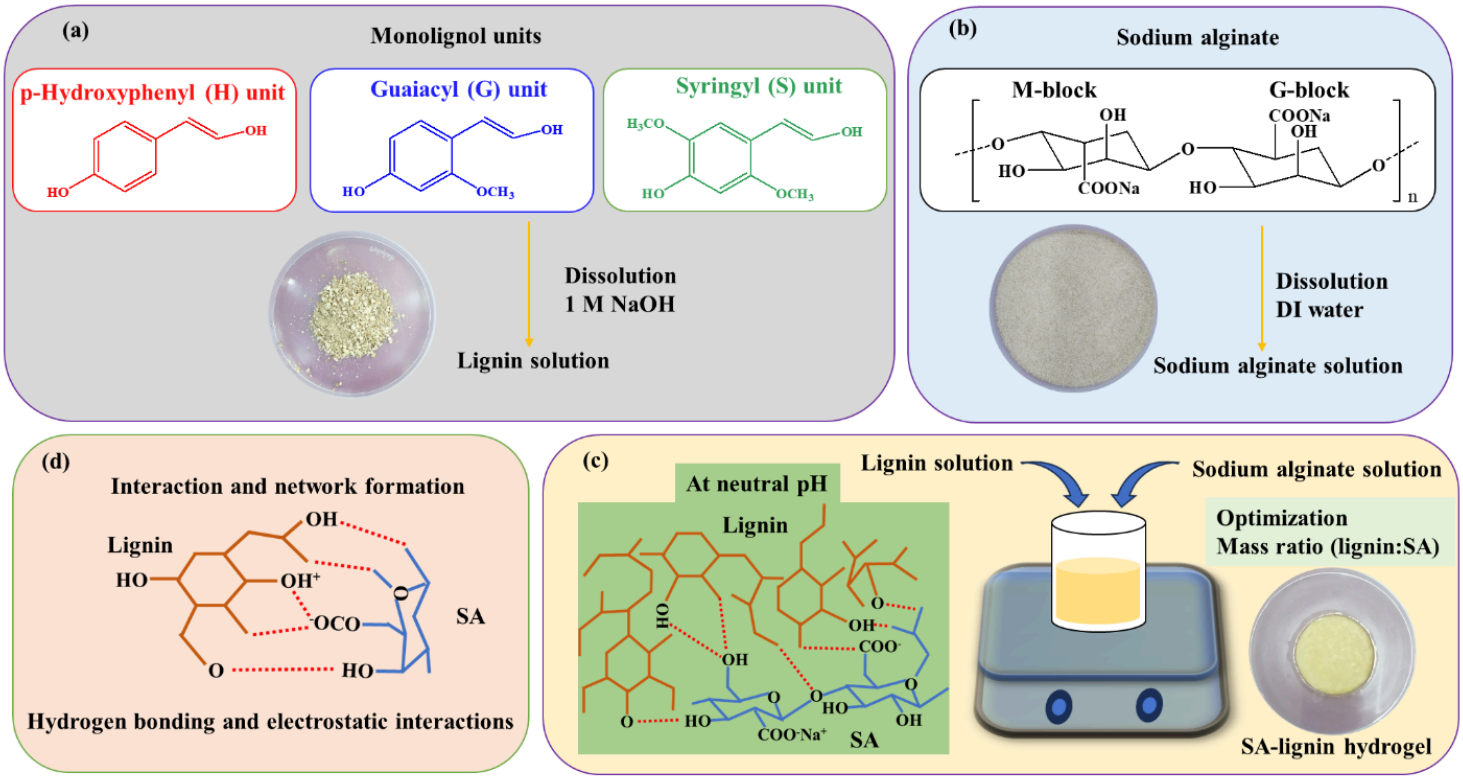

Figure 1

Schematic representation for the (a) dissolution of lignin, (b) dissolution of SA, (c) synthesis of SA-lignin hydrogel, and interactions between lignin and SA at neutral pH, and (d) interactions and network formation of lignin and SA through hydrogen bonding and electrostatic interactions

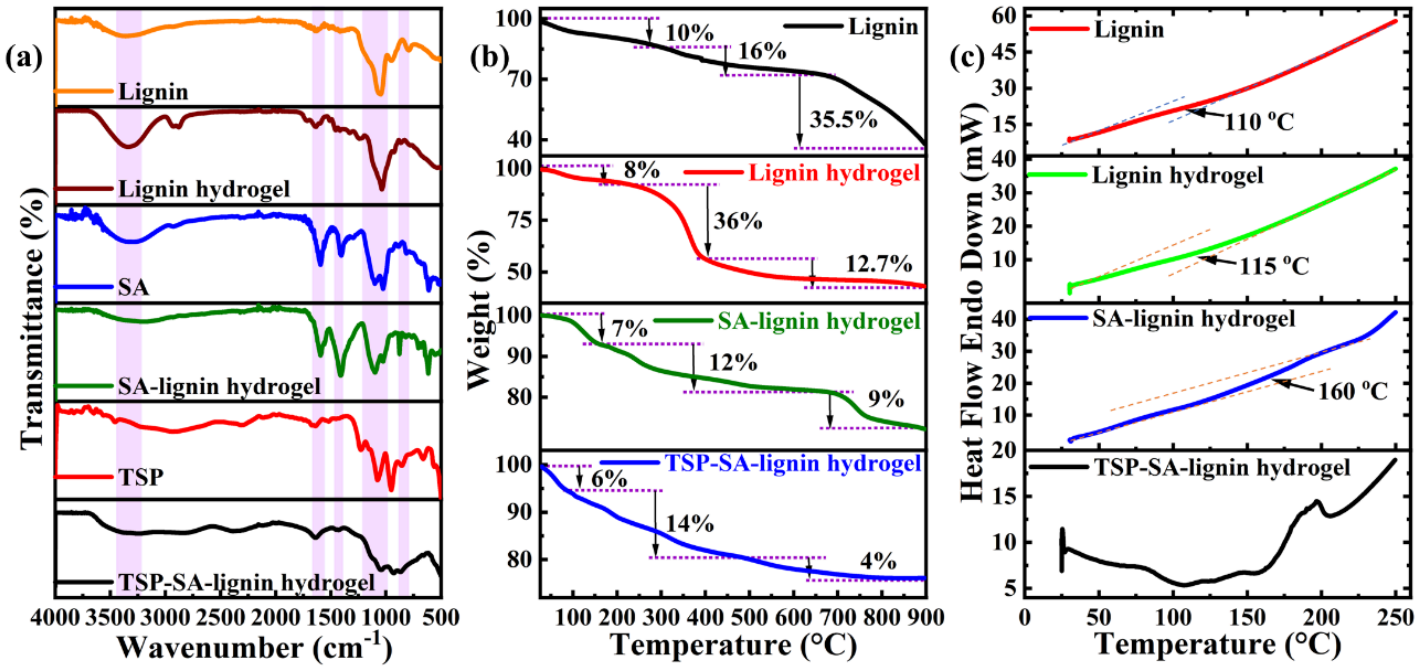

Figure 2

(a) FTIR spectra, (b) TGA, and (c) DSC plot of lignin, lignin hydrogel, SA-lignin hydrogel, and TSP-SA-lignin hydrogel

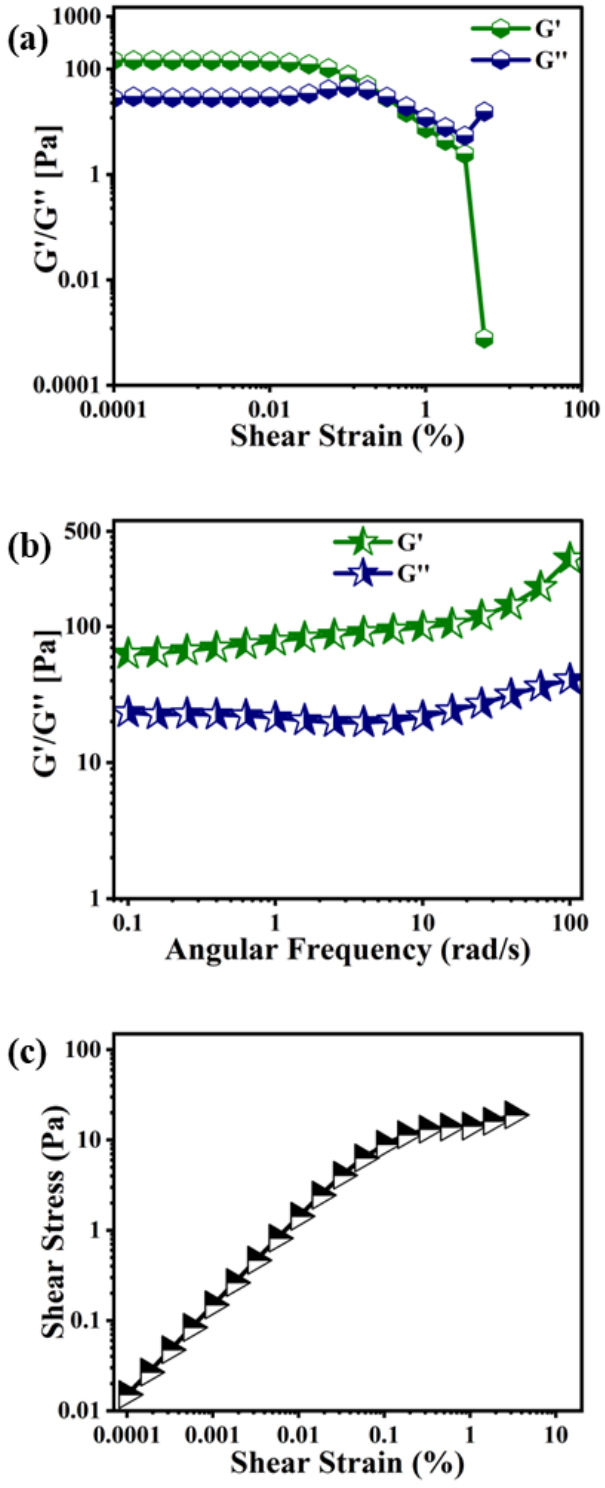

Figure 3

Rheological properties of SA-lignin hydrogel, (a) Modulus vs shear strain, (b) Modulus vs angular frequency, (c) Shear stress vs shear strain

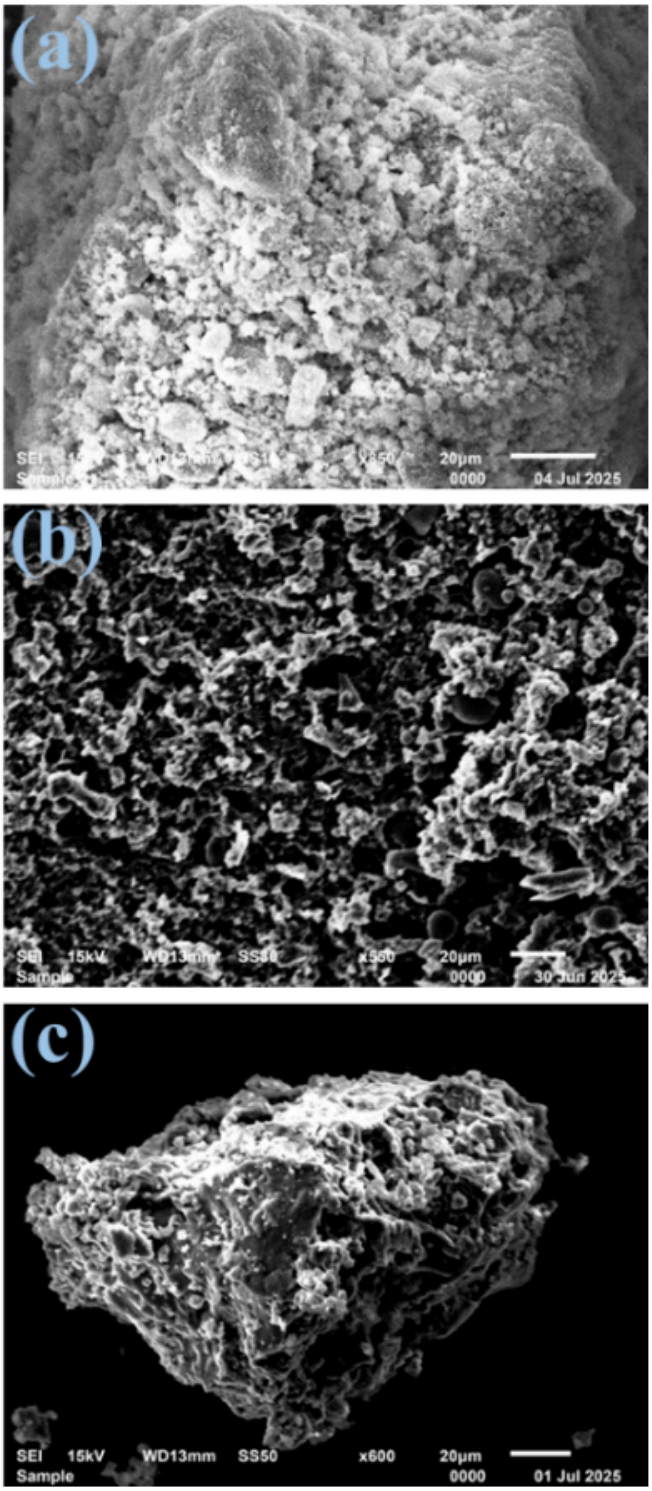

Figure 4

SEM images of (a) lignin, (b) lignin hydrogel, and (c) SA-lignin hydrogel

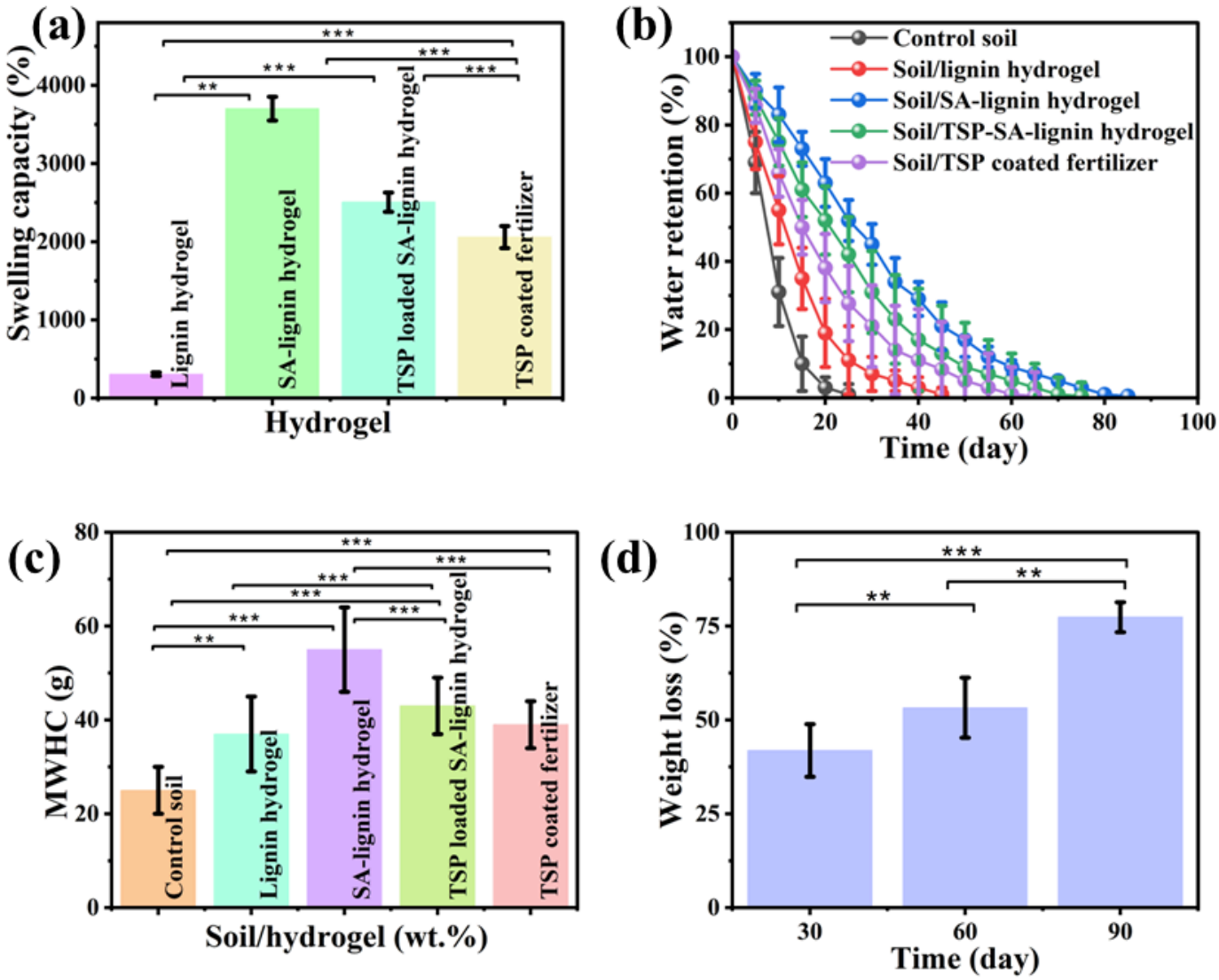

Figure 5

(a) Swelling capacity of lignin hydrogel, SA-lignin hydrogel, TSP-loaded SA-lignin hydrogel, and TSP-coated fertilizer. (b) Water retention of control soil, soil/lignin hydrogel, soil/SA-lignin hydrogel, soil/TSP-loaded SA-lignin hydrogel, and soil/TSP-coated fertilizer. (c) MWHC of control soil, soil/lignin hydrogel, soil/SA-lignin hydrogel, soil/TSP-loaded SA-lignin hydrogel, and soil/TSP-coated fertilizer. (d) Biodegradation study of SA-lignin hydrogel weight loss during 90 days of soil burial incubation. Asterisks denote statistically significant differences between groups (*p < 0.05, **p < 0.01, ***p <0.001).

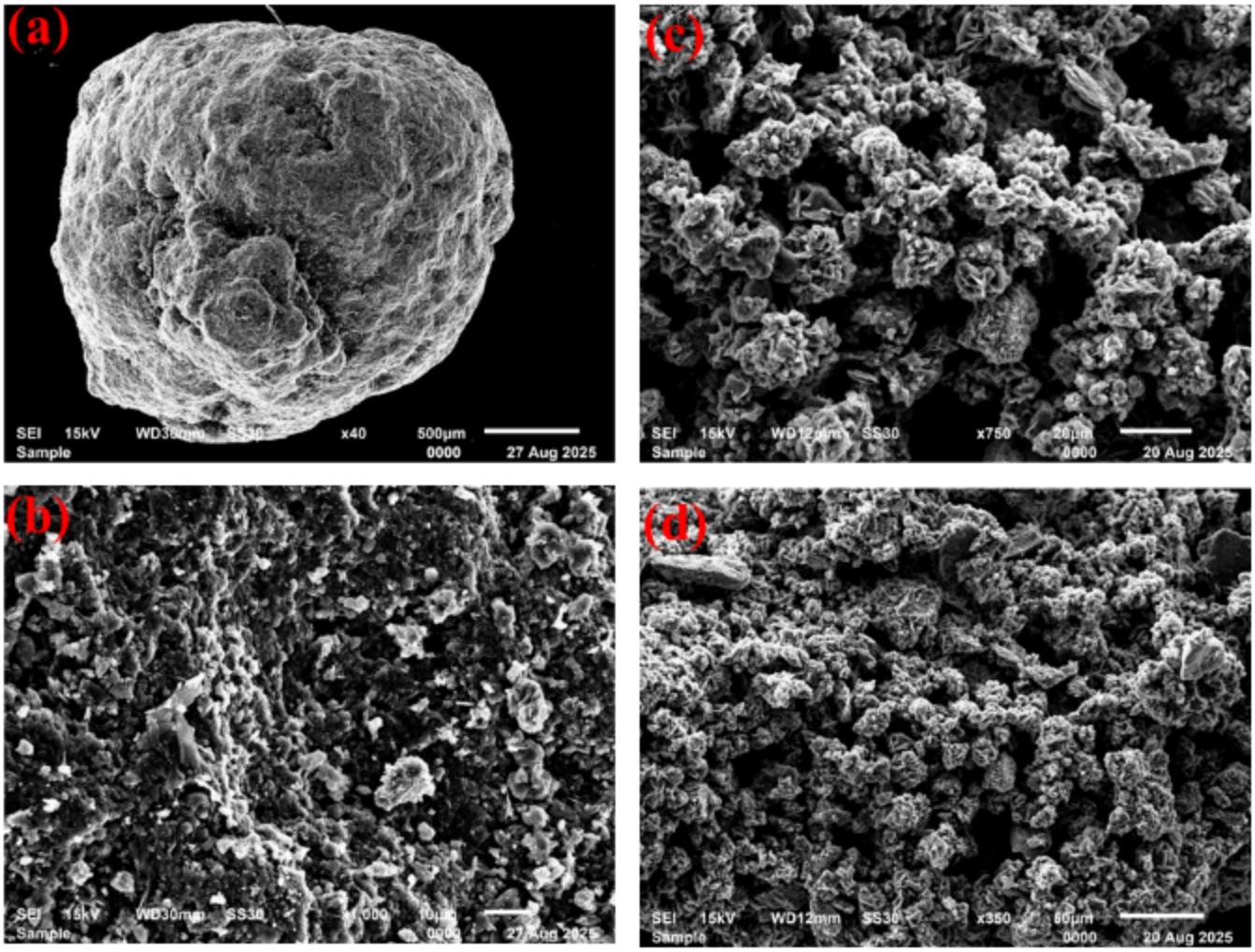

Figure 6

SEM images of (a) pure TSP granule, (b) pure TSP surface, (c, d) TSP-loaded SA-lignin hydrogel (in situ method)

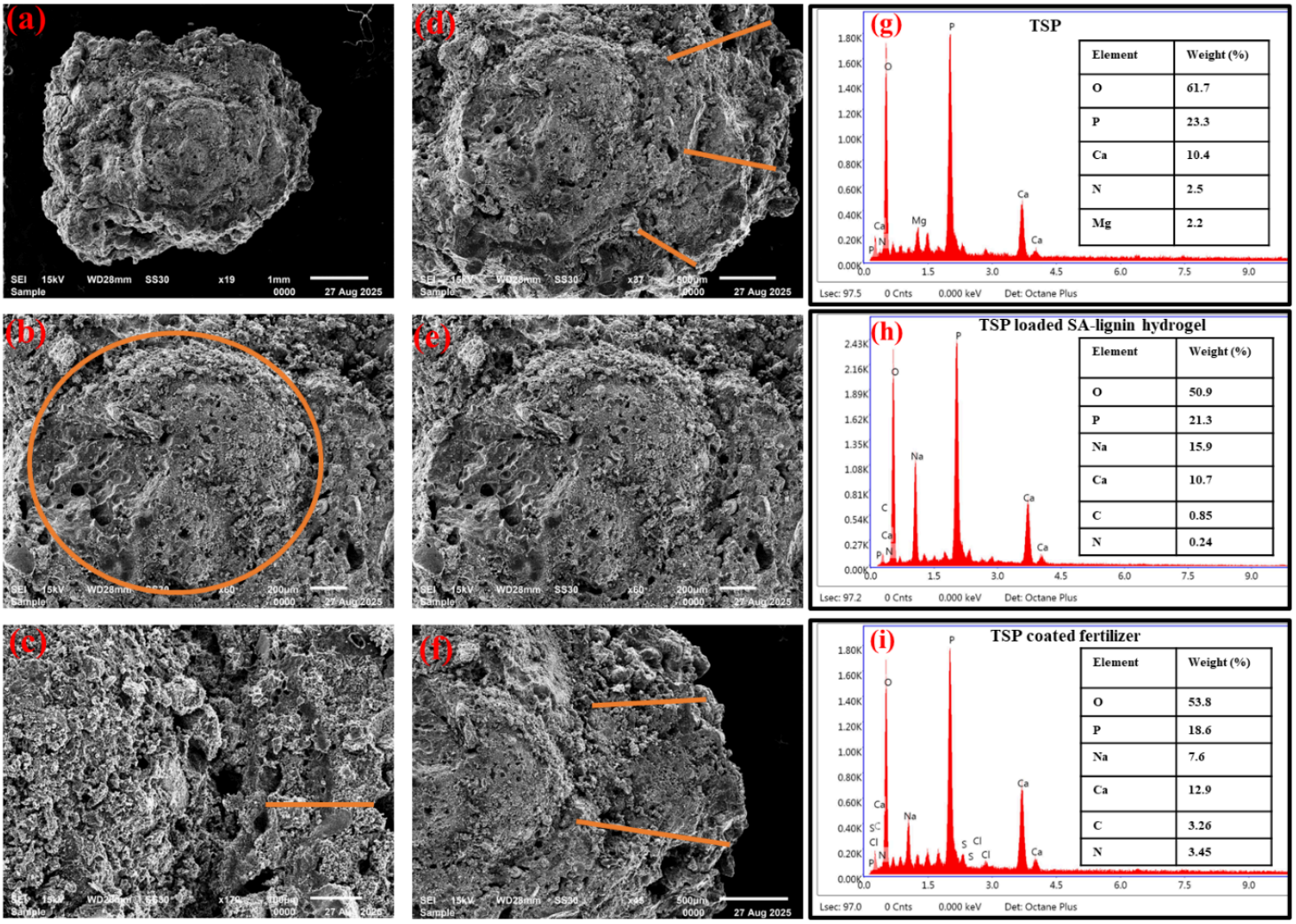

Figure 7

(a-f) Cross-sectional SEM images of TSP-coated fertilizer (coated with SA-lignin hydrogel); and (g-i) EDX with elemental composition of TSP, TSP-loaded SA-lignin hydrogel, TSP-coated fertilizer with SA-lignin hydrogel

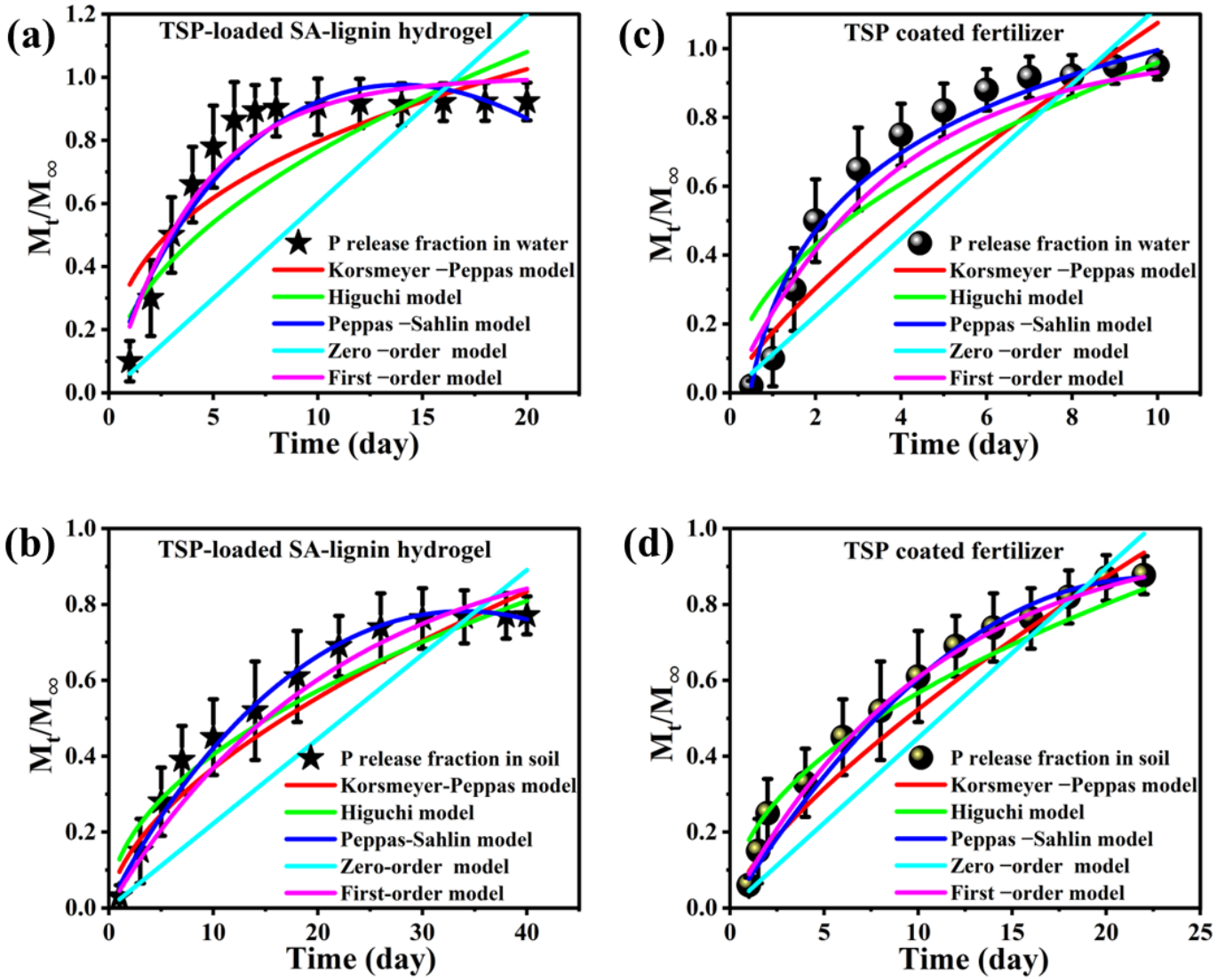

Figure 8

Empirical kinetic models used in the determination of release mechanisms in the phosphorus release studies in DI water and soil; (a) phosphorus release in DI water from TSP-loaded SA-lignin hydrogel, (b) phosphorus release in soil from TSP-loaded SA-lignin hydrogel, (c) phosphorus release in DI water from TSP coated fertilizer, and (d) phosphorus release in soil from TSP coated fertilizer